The $C_4H_4^{\bullet+}$ Potential Energy Surface. 3. The Reaction of Acetylene with Its Radical Cation

Vojtěch Hrouda,[†] Martina Roeselová,[†] and Thomas Bally*

Institute of Physical Chemistry, University of Fribourg, Pérolles, CH-1700 Fribourg, Switzerland

Received: December 16, 1996; In Final Form: February 28, 1997[⊗]

The reaction of acetylene (Ac) with its radical cation ($Ac^{\bullet+}$) is studied at the CCSD(T)/cc-pVTZ//QCISD/6-31G* level of theory and by the B3LYP/6-31G* density functional method. Contrary to earlier claims, we find that vertical ionization of the neutral acetylene dimer leads to a bound state which relaxes to a T-shaped ion−molecule complex 8.3 kcal/mol below the separated fragments. Once Ac and $Ac^{\bullet+}$ have approached to less than an ≈3 Å center to center distance, spin and charge begin to delocalize and the complex collapses smoothly to the cyclobutadiene radical cation (CB) via a linear complex (LC1) and/or a cyclopropenylcarbene cation (CC). Rearrangements to other stable $C_4H_4^{\bullet+}$ isomers require H shifts which are promoted by localization of the positive charge on one C atom. From LC1 this leads directly to the transition state LC2 for formation of a pivotal intermediate, $H_2C{=}C{=}CHCH^{\bullet+}$ (methyleneallene, MA), which in turn collapses with $E_a \approx 3$ kcal/mol to the methylenecyclopropene radical cation (MCP), the most stable $C_4H_4^{\bullet+}$ isomer. Additional [1,2] H shifts which require higher activation energies lead to the radical cations of butatriene (BT, E_a ≈17 kcal/mol from MA) or vinylacetylene (VA, $E_a \approx 20$ kcal/mol from MA) which are of stability similar to that of CB. These findings are in accord with condensed phase experiments on alkylated acetylenes, where the corresponding CB derivatives were the only products observed. However, in gas phase studies other $C_4H_4^{\bullet+}$ isomers were observed in Ac + $Ac^{\bullet+}$ reactions. Perhaps these arise through bifurcations leading to structures with localized charge without passing through the stationary points located in this study. B3LYP/6-31G* results were found to be in close agreement with the reference coupled cluster calculations for most parts of the $C_4H_4^{\bullet+}$ potential energy surface probed in this study. However, it should be noted that density functional methods may give a wrong dissociation behavior for radicals because they fail to localize the spin (and the charge in the present case) when this is required and therefore cannot be used in the loosely bound region for ion−molecule complexes.

1. Introduction

In the first paper of this series describing structures and rearrangements on the $C_4H_4^{\bullet+}$ potential energy surface we had focused on the cyclobutadiene radical cation (CB) and its Jahn−Teller (JT) distortion.[1] In the second paper, the JT effect in the tetrahedrane radical cation and its facile rearrangement to CB was discussed,[2] whereas the present study traces the continuation of our program for investigating mechanisms of ion−molecule reactions[3] such as they occur in condensed phase and/or in gas phase experiments. Thus, we will investigate the pathways for the reaction of acetylene (Ac) with its radical cation ($Ac^{\bullet+}$) and the stable products formed therefrom.

Upon diffusion in the *condensed phase*, the radical cations of alkylated acetylenes were found to react spontaneously with their neutral parent compounds to form cyclobutadiene radical cations (CBs).[4] This is in contrast to many olefinic and aromatic hydrocarbons M where the reaction usually stops at the stage of the sandwich complexed dimer radical cations $(M)_2^{\bullet+}$ which show distinct spectroscopic features.[5] In the case of dialkylacetylenes, the resulting CBs (*cf.* Scheme 1) were identified by comparison of their ESR spectra with those of the same species prepared independently by photolysis of $AlCl_3$ complexes. Interestingly, upon annealing of Freon matrices containing CBs formed from alkylacetylenes, propargyl radicals HC≡CCHR arise as the sole paramagnetic products.[6] This implies that alkyl-CBs redissociate spontaneously upon loss of a β-proton, a proposition which would seem to require some substantiation.

SCHEME 1: Condensed Phase Ion−Molecule Chemistry of Acetylene

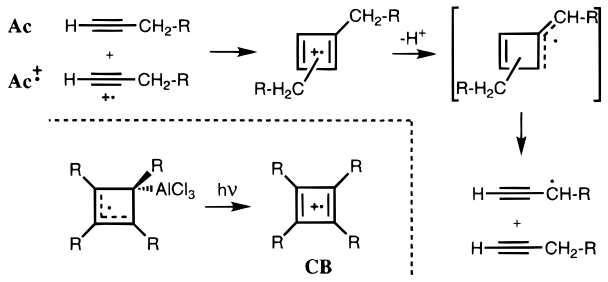

On the other hand, the Ac + $Ac^{\bullet+}$ reaction is one of the best studied *gas phase ion−molecule reactions* which was investigated by a wide range of techniques over the past 40 years.[7] Most of this work was done at low pressures, where mainly the fragments $C_4H_3^+$ and $C_4H_2^{\bullet+}$ were observed. The dependence of their ratio on the incident energy allowed a modeling of the kinetics by statistical theories, but since, in these experiments, the ground state potential energy surface of $C_4H_4^{\bullet+}$ is not directly probed, we will not comment in any detail on these studies.[7b] Conversely, in early high-pressure studies the primary cation $C_4H_4^{\bullet+}$ was formed in a reaction which was found to follow third order kinetics (*i.e.*, required stabilization by collision with a molecule of neutral acetylene).[9]

Recently, attention returned to the ion−molecule chemistry of acetylene due to its importance in soot formation of acetylene-rich flames[10] and the discovery of unsaturated hydrocarbon cations in interstellar clouds.[11] In this perspective, the title reaction was studied in an ion-flow tube at 0.3-0.4 Torr, which

[†] On leave from the J. Heyrovskỳ Institute of Physical Chemistry, Academy of Sciences of the Czech Republic, Prague.

[⊗] Abstract published in *Advance ACS Abstracts,* April 15, 1997.

S1089-5639(96)04079-0 CCC: $14.00

SCHEME 2: Gas Phase Ion−Molecule Chemistry of Acetylene

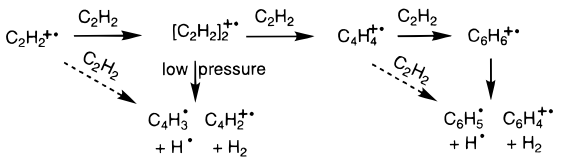

also permitted probing of the nature of the primary $C_4H_4^{\bullet+}$ species.[12] Interestingly, *two isomeric forms* of this cation were formed from Ac + $Ac^{\bullet+}$ which showed distinct reactivity toward neutral acetylene or benzene. By analogy with similar behavior of $C_4H_4^{\bullet+}$ formed from vinylacetylene,[13] it was concluded that the more reactive population corresponds to a linear structure (vinylacetylene) and the less reactive one to a cyclic structure (usually presumed to be the methylenecyclopropene cation). They did not consider the possible formation of CB which could nowadays be identified quite unambiguously by neutralization−reionization mass spectrometry[14] or by its distinct reactivity toward thiophene and allene.[15]

The Ac + $Ac^{\bullet+}$ reaction was also probed in *ionized acetylene clusters* in an effort to mechanistically distinguish the formation of fragments via a collision complex $(C_2H_2)_2^{\bullet+}$ (solid arrows in Scheme 2) or directly (dashed arrows). In 1982, Ono and Ng measured appearance energies of $(C_2H_2)_2^{\bullet+}$ (10.44 eV) and $(C_2H_2)_3^{\bullet+}$ (9.83 eV) as well as those of some fragment cations obtained by photoionization of molecular beams containing small acetylene clusters.[8] However, Booze and Baer recently demonstrated by a coincidence experiment that *direct* photoionization of acetylene clusters is impossible,[16] and they concluded that the $(C_2H_2)_2^{\bullet+}$ and $(C_2H_2)_3^{\bullet+}$ observed by Ono and Ng must have arisen from the next higher neutral homologues (trimers and tetramers, respectively) which may stabilize themselves by loss of a neutral acetylene molecule upon ionization.[17]

Booze and Baer used quantum chemical calculation to rationalize the impossibility of obtaining $(C_2H_2)_2^{\bullet+}$ by direct photoionization of the T-shaped neutral dimers. They found very different equilibrium structures for the neutral and the ionized acetylene dimer from which they concluded that Franck−Condon factors for photoionization to bound vibrational states of the dimer cation should be vanishingly small. Moreover, their calculations indicated that vertical ionization of the neutral dimer leads to a state which decays spontaneously to C_2H_2 + $C_2H_2^{\bullet+}$ and therefore cannot be observed unless a mechanism for the dissipation of the excess energy (such as monomer evaporation from a larger cluster) is available.[16] Interestingly, they found *two different* structures for $(C_2H_2)_2^{\bullet+}$, depending on whether the optimization started from the vertically ionized dimer or the trimer (which spontaneously loses a C_2H_2 on relaxation). Booze and Baer did not comment on this interesting finding (*cf.* Scheme 3) which we will reexamine in the present study.

On the other hand, Tachikawa *et al.*[6] attempted to substantiate the interpretation of their ESR data by quantum chemical calculations on alkylated acetylene dimer cations. Thereby they found two different states of the dimer cations which they call σ- and π-types according to the character of the singly occupied MO (SOMO). The π-cations represent tightly bound CB-type structures, whereas the σ-cations correspond to loosely bound charge−resonance-type dimer cations which are, however, ≈2 eV less stable. Reaction path calculations led them to the interesting conclusion that the methylacetylene dimer cation collapses to the less stable *cis*-dimethyl-CB because the path to the 0.54 eV more stable trans form requires a larger activation

SCHEME 3: Ionized Cluster Chemistry of Acetylene

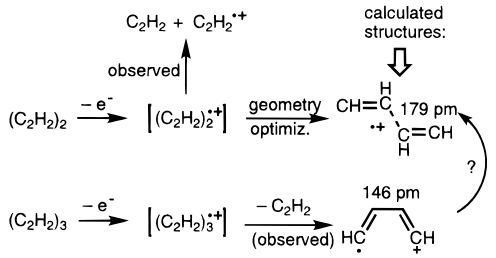

energy. Unfortunately, Tachikawa *et al.* give very little information on how they carried out their geometry optimizations (symmetry constraints, characterization of stationary points) which makes it difficult to judge the validity of their propositions that will have to be examined critically.

Very recently, Zhu *et al.*[19] exploited the fact that the potential energy surfaces for cluster cations are usually quite similar to those of Rydberg states of the neutral clusters. Thus, they found that (a) the Δ_g Rydberg states of $(C_2H_2)_2$ are stable (unless the C≡C stretching vibration is excited) and (b) subsequent ionization yields $(C_2H_2)_2^{\bullet+}$ with no concomitant fragmentation. From this they concluded that the dimer cation must have a stable geometry which is perhaps preformed in the Rydberg state.

It is the purpose of the present computational study to provide a coherent picture of the potential energy surface for the reaction of acetylene with its radical cation and the subsequent rearrangement to tightly bound $C_4H_4^{\bullet+}$ species. Thereby we will address the following questions:

(a) What is the pathway for the C_2H_2 + $C_2H_2^{\bullet+}$ reaction under conditions where the excess energy can be efficiently dissipated (condensed phase and high-pressure gas phase experiments)? In particular, what are the activation barriers for conversion of loosely bound to various tightly bound $C_4H_4^{\bullet+}$ species?

(b) Is it possible that different stable $C_4H_4^{\bullet+}$ isomers are formed concomitantly in the C_2H_2 + $C_2H_2^{\bullet+}$ reaction?

(c) Does ionization of neutral acetylene dimer lead to a bound species, and if yes, why was this species not observed by direct photoionization?

(d) How conclusive are the results of the previous quantum mechanical studies on the title subject?

Although we will perhaps not be able to definitively resolve all of the above problems, we believe that application of state-of-the-art quantum chemical techniques can provide important insight into ion−molecule reactions in general and that of acetylene in particular. We will presently limit ourselves to the parent C_2H_2 + $C_2H_2^{\bullet+}$ system, but an extension of this study to include the experimentally investigated methyl derivatives is straightforward and will be presented later.

2. Computational Methods

The methodology used in the present study is similar to that described in some detail in the previous paper.[2] Therefore we limit ourselves to a brief summary and focus on those aspects which differ. Initially, all structures were optimized at the restricted open shell Hartree−Fock (ROHF) level. Subsequently, they were reoptimized by the spin unrestricted variants of the B3LYP density functional[20] and the QCISD methods[21] using the standard 6-31G* basis set.[22] All stationary points were characterized by Hessian calculations at the above levels.

In addition, in the case of transition states, intrinsic reaction coordinate (IRC) calculations[23] were carried out systematically at the B3LYP/6-31G* level to ascertain the identity of the minima which they interconnect. The loose complexes were

TABLE 1: Optimized Geometry, Binding Energy (ΔE), and 0 K Binding Energy (ΔE_0, in kcal mol^{-1}) of the Neutral T-Shaped Complex $(C_2H_2)_2$

	HF		B3LYP			QCISD		CCSD(T)	
	6-31G*	6-31++G*	6-31G*	6-31++G*	cc-pVTZ	6-31G*	6-31++G*	cc-pVTZ[a]	expt[b]
E[c]	−153.637 68	−153.647 46	−154.653 95	−154.667 78	−154.728 50	−154.169 71	−154.181 38	−154.377 54	
r_0[d]	2.968	3.070	2.724	2.797	2.835	2.733	2.731		2.743
R(C≡C)[e]	1.186	1.189	1.206	1.208	1.197	1.213	1.215		1.203
R(C−H)[e]	1.057	1.058	1.067	1.068	1.062	1.069	1.070		1.062
ΔE	−1.27	−0.79	−1.67	−0.98	−0.87	−1.77	−1.67	−1.47	
ΔE_{corr}[f]	−0.83	−0.70	−1.07	−0.80	−0.79	−0.93	−0.80	−1.25	
$\Delta E_{0,corr}$[g]	−0.46	−0.33	−0.70	−0.43	−0.42	−0.56	−0.43	−0.88[h]	

[a] Single point calculation at QCISD/6-31G* geometry. [b] Ref 29, intramolecular bond lengths from isolated acetylene. [c] Total energies in hartrees. [d] Distance between donor H atom and center of acceptor acetylene. [e] Both C≡C and all C−H bond lengths equal within >0.001 Å with the exception of the donor C−H bond which is longer by 0.001−0.003 Å. [f] Value corrected for the basis set superposition error. [g] Values corrected for differences in zero-point energies and basis set superposition error, calculated at the respective level, except where noted. [h] ΔZPE = 0.37 kcal mol^{-1} taken from the frequencies calculated at the B3LYP/cc-pVTZ level.

also reoptimized with a basis set containing diffuse functions (6-31++G*). Finally, single point energies were evaluated at the QCISD geometries by the UCCSD(T) method[24] using Dunning's correlation-consistent triple ζ (cc-pVTZ) basis set.[25] Zero-point energies (ZPEs) for the evaluation of $\Delta E_0 = \Delta E + \Delta$ZPE were taken from frequencies calculated at the level used for the geometry optimization. ΔE from CCSD(T) calculations were supplemented by ΔZPE from QCISD frequencies. Basis set superposition errors (BSSEs) were calculated by the Boys−Bernardi procedure[26] for the loose complexes, *i.e.*, those in which no new C−C σ-bonds have developed.

We checked for the appropriateness of using single-determinant reference wave-functions by carrying out CAS(7,8) calculations on the stationary points. In all cases, the CASSCF wavefunction was described to ≥87% by the ground state reference determinant and no individual excited configuration contributed by ≥3%. The expectation value $\langle S^2 \rangle$ in the unrestricted Hartree−Fock (UHF) reference determinants was <0.77 in the B3LYP calculations. In the reference UHF wavefunctions used in the QCISD and CCSD(T) calculations, $\langle S^2 \rangle$ showed significant deviations from 0.75, especially at transition states where it exceeds 0.9. However, as shown by Stanton,[27] even substantial contamination by higher spin states is effectively removed at the CCSD (or QCISD) level unless bonds are stretched very far from their equilibrium lengths.

All calculations were carried out with the Gaussian94 suite of programs[28] on an SGI Power Challenge server, with the exception of the CCSD(T)/cc-pVTZ jobs which were run on a NEC SX-3 vector machine.

3. Results and Discussion

3.1. The Neutral Dimer. Before going into the discussion of ion−molecule complexes, we recall some pertinent features of the neutral acetylene dimer $(Ac)_2$ (Scheme 4) which was investigated in some detail by microwave and rotationally resolved IR spectroscopy.[29a,b] The data obtained in these studies were successfully modeled in terms of a hydrogen-bonded T-shaped structure TN which undergoes, however, a rapid tunneling automerization by simultaneous rotation of the monomers around parallel axes at a gigahertz rate.

This model received support from MP2/DZP calculations which showed TN to be an energy minimum, whereas the parallel structure is a transition state for the automerization process.[29c] We decided to recalculate TN with our present methodology as a basis for our study of ionized acetylene dimers. The results are presented in Table 1, which shows that the structure and binding energy of TN depend surprisingly little on the presence or absence of diffuse functions in the basis set and/or on the recovery of correlation energy. We conclude from this that dispersive interactions (which are pure correlation effects and hence cannot be modeled at the Hartree−Fock level) are of minor importance and that the binding in TN is predominantly by acid−base (or donor−acceptor) interactions which lead also to a substantial dipole moment of 0.28 D.[29a]

SCHEME 4: Neutral Acetylene Dimer

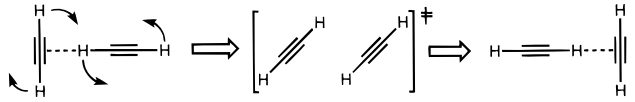

We note that the B3LYP/6-31G* geometry is in very good accord with experiment and with that obtained at the QCISD level, and the binding energy of 0.7 kcal/mol is only 0.18 kcal/mol lower than that obtained by the (very expensive) CCSD(T)/cc-pVTZ calculation. This was unexpected in view of recent studies demonstrating that density functional methods are poorly suited for calculating van der Waals type as well as hydrogen-bonded complexes.[30] Addition of diffuse functions or going from DZ to TZ basis sets results mainly in the expected decrease of the basis set superposition error, except at the QCISD level, but as the binding energies decrease simultaneously, the corrected values do not differ much from those obtained with smaller basis sets.

A comment is in order with regard to zero-point energies and thermal corrections which require a correct description of the vibrational structure. As noted by Handy *et al.*[31] a faithful modeling of the bending vibrations of π-bonded systems requires large AO basis sets containing at least f functions in addition to a good account for correlation energy. Indeed, all methods gave bending frequencies of acetylene which were too low by 10−20%, and therefore we decided to calculate the frequencies for differences in zero-point energies and thermal corrections of reactions involving Ac, $Ac^{\bullet+}$ or loosely bound complexes of the two with the cc-pVTZ basis set at the B3LYP level, which has proven very reliable in this respect.[32]

3.2. The Dimer Cation. In dimer radical cations composed of identical π-systems, attractive forces usually occur in the form of covalent interactions which can be thought to arise through charge resonance $M^{\bullet+}-M \leftrightarrow M-M^{\bullet+}$ or through interaction of the two HOMOs which contain a total of three electrons.[33] This requires optimal overlap between the π MOs, and therefore the most stable form of π dimer cations is often of a sandwich type or has at least one long bond formed by a pair of facing p_π AOs, as in the case of the $(ethylene)_2^{\bullet+}$ linear complex.[3,34] As will be shown below, such a structure is indeed formed eventually also in the case of $(Ac)_2^{\bullet+}$.

However, at center-to-center distances of >3.8 Å the same mode of bonding which prevails in TN appears to be the most favorable one in $(Ac)_2^{\bullet+}$. In fact, optimization of TN after

TABLE 2: Energy Differences (ΔE) and 0 K Binding Energies (ΔE_0, in kcal mol^{-1}) Relative to Separated Fragments of Weakly Bonded Complexes on the $C_4H_4^{\bullet+}$ Potential Energy Surface

$C_4H_4^{\bullet+}$ structure[a]		ROHF 6-31G*	ROHF 6-31++G* [b]	B3LYP 6-31G*	UQCISD 6-31G*	UCCSD(T) cc-pVTZ[c]
Ac + Ac$^{\bullet+}$	E[d]	−153.278 64	−153.284 49	−154.247 62	−153.772 40	−153.960 65
	ZPE[e]	36.33	36.27	33.06	32.41	32.41
PC	ΔE	−18.00	−15.49	−41.09	−30.09	−32.97
	ΔE_{corr}[f]	−17.01	−15.27	−39.97	−27.17	−32.12
	$\Delta E_{0,corr}$[g]	−16.13	−14.48	−38.99	−26.11	−31.06
TC	ΔE	−8.63	−7.19	*h*	−10.15	−9.97
	ΔE_{corr}[f]	−8.09	−7.01		−8.69	−9.54
	$\Delta E_{0,corr}$[g]	−7.30	−6.27		−7.45	−8.30
TC//TN[i]	ΔE	−3.37	−2.43	*h*	−5.24	−5.07
	ΔE_{corr}[f]	−2.94	−2.31		−4.43	−4.86

[a] For optimized structures see Figure 5. [b] Numbers used in the construction of Figures 1 and 2. [c] Single point calculations at QCISD geometries. ZPEs are also taken from QCISD calculation. [d] Total energies in hartrees. [e] Zero-point vibrational energy in kilocalories per mole. [f,g] See corresponding footnotes in Table 1. [h] No binding at the B3LYP level; for discussion see text. [i] TC at the geometry of TN.

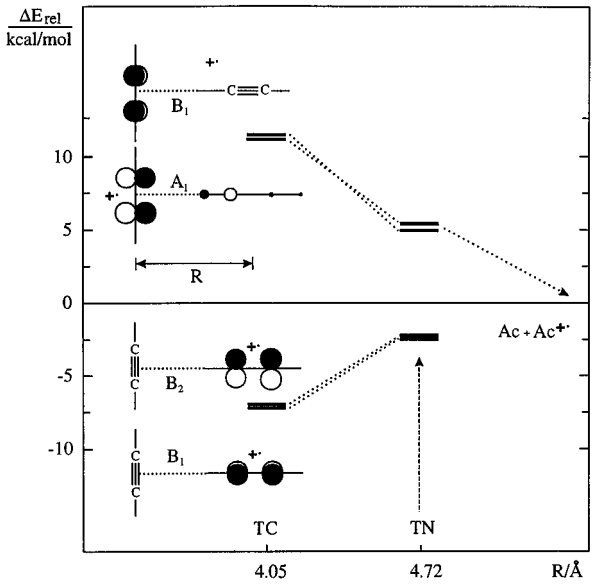

Figure 1. ROHF/6-31++G* energies and HOMOs of the four lowest electronic states of the T-shaped complex between acetylene and its radical cation at the equilibrium geometry of the neutral (TN) and the cation (TC), relative to the separated fragments. In the ground state of TC spin and charge are localized on the H-bonding acetylene (the one to the right in the drawings). Note that the binding energy of TC increases considerably on going to correlated levels of theory (*cf.* Table 2).

removal of an electron leads at all levels of theory (except B3LYP, see below) to an energy minimum which retains the structural features of TN and will hence be called TC (*cf.* Figure 1). Whereas vertically ionized TN is bound by only ≈4 kcal/mol, this increases to ≈8 kcal/mol in TC (*cf.* Table 2). This finding is in sharp contrast to Booze and Baer's[16] who claimed that TC lies about 7 kcal/mol *above* the separated fragments and concluded that TN dissociates spontaneously on ionization. However, they also reported that the charge in vertically ionized TN was located on that monomer which does *not* engage in H-bonding, whereas we found the opposite.

Apparently, the calculation of vertically ionized TN by Booze and Baer had converged to an *excited state.* As this state has a different symmetry in C_{2v}, we recalculated it with the 6-31++G* basis set and found it to lie indeed ≈5 kcal/mol *above* the separated fragments. In fact, one can calculate four distinct states of the T-shaped dimer cation which differ in the nature of the singly occupied π HOMO, as shown in Figure 1. Not unexpectedly, they are pairwise nearly degenerate, and the splitting between those which carry spin and charge on different acetylene moieties (and hence the binding energy in the $^2B_1$ ground state) increases with decreasing distance. Thus, we conclude that if TN is ionized at threshold, the resulting dimer cation should be weakly bound and under high-pressure conditions it should collapse to the more strongly bound TC.[35]

If the intermolecular distance in TC is decreased below the equilibrium value of ≈4 Å, the energy increases sharply when C_{2v} symmetry is maintained (see dotted line joining solid circles in Figure 2). On unconstrained geometry optimization, the H-bonding acetylene moiety begins to escape the repulsion by the π-cloud of the other by tilting upward, whereby a transition state TS0 is reached. Shortly thereafter the charge and spin begin to delocalize and, if C_s symmetry is maintained, the system eventually collapses to a perpendicular complex PC of D_{2d} symmetry. This "perpendicular" mode of interaction is also bonding at >2.5 Å, but less so than that of the T-shaped dimer which wins at longer distances. On further reduction of the intermolecular distance, the ground state of PC correlates in D_{2d} with a highly excited state of tetrahedrane radical cation (dotted line joining solid triangles in Figure 2), which is of no relevance in the present study.[2]

When we wanted to recompute the potential energy curves by the B3LYP method, we noted that, irrespective of the distance R and the symmetry, spin and charge were always delocalized over both acetylene moieties, which led to a very strange dissociation behavior, as documented in Figure 3 on the example of the D_{2d} pathway: whereas the ROHF curve leads smoothly to the dissociation limit, the B3LYP curve begins to fall off in the region where spin and charge localize in ROHF and does not converge at all to the energy of the separated fragments (which is furthermore much too high). Thus, DFT methods do not seem to be appropriate for the calculation of dissociations of species where charge or spin must localize on one fragment,[36] but this does not preclude B3LYP from giving predictions in good accord with QCISD calculations for both geometries and energies of more tightly bound species (see below).

However, the localization of spin and charge in PC (or other weakly bound complexes) can certainly not be modeled correctly at the Hartree−Fock level; *i.e.*, dynamic correlation is expected to play an important role here. Therefore, we recomputed the energy of PC by the CISD method,[37a] which gave the curve joining the open squares in Figure 3. Obviously, ROHF had underestimated the binding energy of PC by about 30% relative to CISD[37b] (and by even more relative to our reference level, CCSD(T) /cc-pVTZ), which proves that correlation plays an important role in shaping the potential energy surface for the dissociation of ion−molecule complexes.

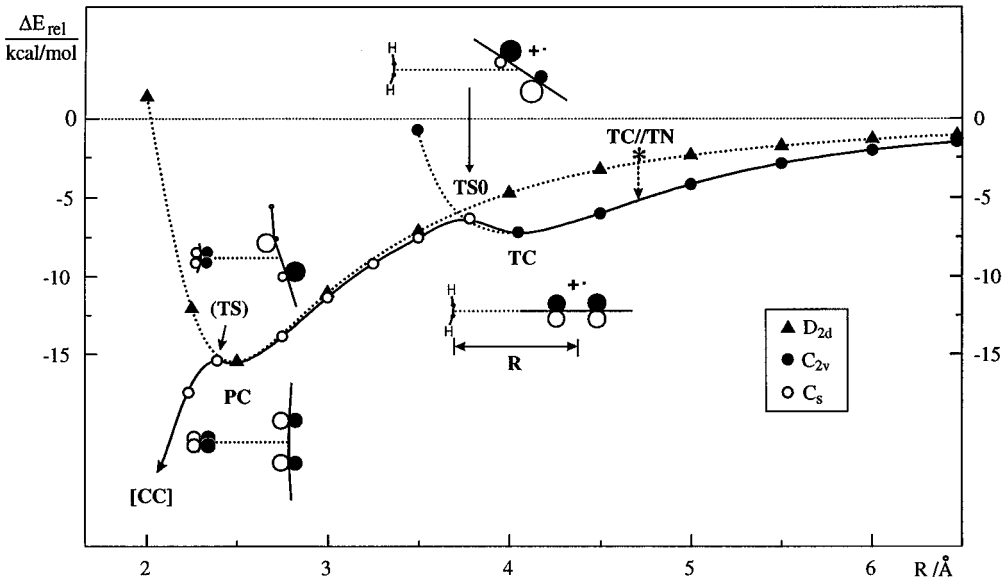

Figure 2. ROHF/6-31++G* potential energy surfaces (energies relative to separated fragments) for the interaction of acetylene and its radical cation as a function of the center-to-center distance *R* (i) in a perpendicular approach of D_{2d} symmetry (dotted line joining solid triangles) and (ii) for an approach through a H-bonded complex of C_{2v} symmetry (TC, full circles) which collapses via a tilted structure of C_s symmetry (open dots) to a perpendicular complex PC of D_{2d} symmetry. TC//TN denotes TC at the geometry of TN. Each mark corresponds to a fully optimized geometry within the given symmetry. The solid line denotes the minimum energy pathway for the formation of $C_4H_4^{\bullet+}$. MO pictures denote the singly occupied HOMO in the respective states.

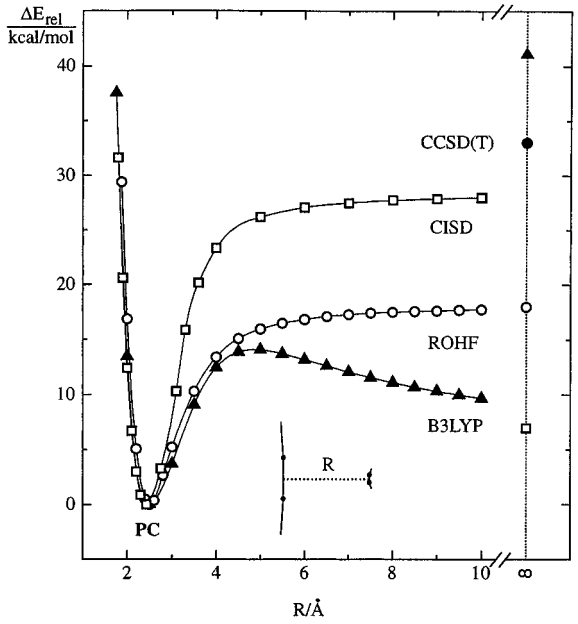

Figure 3. Energy vs center-to-center distance *R* for the dissociation of PC along a C_{2v} pathway by different methods (always with the 6-31G* basis set). The values at infinity are energies of the separated fragments Ac and $Ac^{\bullet+}$ relative to PC (the full circle at infinite distance corresponds to the reference level, *i.e.*, CCSD(T)/cc-pVTZ//QCISD/6-31G*).

Figure 4 shows the degree of localization of the spin and the concomitant increase in the difference between the length of the two acetylene's C≡C bonds in PC in the region of *R* where both change. Both parameters begin to change rather abruptly at ≈2.7 Å (ROHF) or 3.1 Å (CISD) and then converge to their values in the separated fragments within about 1.3 Å (whereas both remain constant over the entire range in B3LYP). Although these changes are not accompanied by any discontinuities in the energies, it is interesting to note that the preference of electron correlation for delocalized wavefunctions delays the onset of localization by ≈0.4 Å.

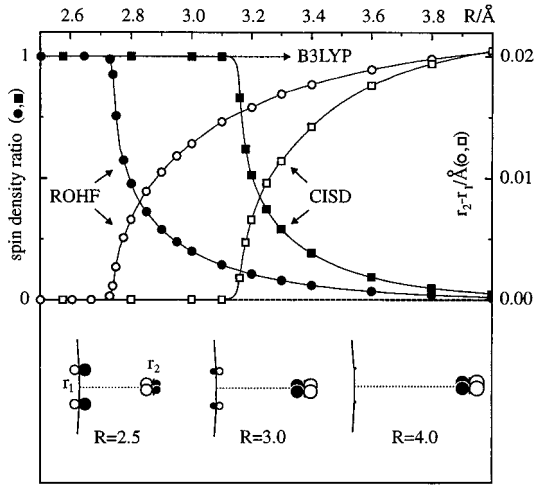

Figure 4. Ratio of spin densities (filled symbols) and difference in C≡C bond lengths (open symbols) of the two acetylene moieties in PC in the region where localization of spin and charge sets in. Note that both parameters remain constant throughout at the B3LYP level (dashed lines). All calculations are with the 6-31G* basis set.

In conclusion, we present the structures (Figure 5) and binding energies of the weakly bound $(Ac)_2^{\bullet+}$ complexes discussed in this section as computed by the different methods with correction for the basis set superposition error and zero-point energy differences (Table 2). We retain from this in particular the ≈5 kcal/mol binding energy of TC at the geometry of TN which increases to ≈9 kcal/mol on relaxation of the ionized complex (slightly less if ZPEs are taken into account, which is not possible at the nonequilibrium TN geometry). This and the fact that TC collapses with a very small activation barrier via PC to more tightly bonded complexes (see below) indicate that it should be possible to form stable $C_4H_4^{\bullet+}$ species by ionization of TN if the excess energy can be dissipated.

Finally we note that B3LYP is not capable of describing the weakly bonded TC complex due to the failure of this model to allow for localization of spin and charge at large intermolecular distances. Conversely, the binding energy of PC appears to be

TABLE 3: Energies (kcal/mol) of $C_4H_4^{\bullet+}$ Structures Relative to CB

$C_4H_4^{\bullet+}$ structure[a]		ROHF/6-31G*		UB3LYP/6-31G*		UQCISD/6-31G*		UCCSD(T)/cc-pVTZ[b]	
		ΔE	ΔE_0	ΔE	ΔE_0	ΔE	ΔE_0	ΔE	ΔE_0
Ac + Ac$^{\bullet+}$		82.80	*77.07*	*c*		87.34	*80.84*	88.02	*81.52*
LC1		66.15[d]	*61.97*[d]	48.82	*44.74*	49.39	*45.42*[e]	49.39	*45.43*[e]
								(49.88)[f]	*(45.92)*[f]
TS1		*g*		50.59	*46.48*	49.91	*45.69*	49.85	*45.63*
CC[h]		45.40	*42.31*	47.97	*44.83*	44.84	*42.16*	45.61	*42.93*
TS2		45.94	*43.17*	48.09	*45.11*	45.43	*43.14*	45.66	*43.38*
LC2[i]		48.40	*44.74*	56.33	*51.40*	56.51	*52.62*	58.77	*54.88*
								(56.89)[f]	*(51.96)*[f]
MA		19.47	*16.78*	25.16	*22.48*	25.37	*23.31*	28.50	*26.45*
TS3		35.91	*32.58*	29.79	*26.50*	31.62	*28.87*	32.44	*29.68*
MCP		−17.92	*−19.27*	−8.52	*−9.50*	−9.52	*−10.10*	−6.69	*−7.27*
TS4		58.18	*52.54*	44.91	*39.63*	49.66	*44.77*	48.18	*43.30*
BT		7.01	*3.50*	−5.06	*−7.09*	0.63	*−1.23*	2.04	*0.17*
TS5		59.75	*54.43*	49.45	*43.73*	55.65	*50.49*	52.06	*46.90*
VA		3.62	*2.24*	−0.63	*−1.70*	1.32	*0.45*	3.46	*2.58*
CB	E[j]	−153.410 59[k]		−154.403 78		−153.911 58[l]		−154.100 92	
	ZPE[m]	42.05		39.01		38.90[l]		(38.90)[n]	

[a] For B3LYP and QCISD optimized structures see Figures 6, 9, and 10; structures TS*x* are transition states at all levels; all other species are minima, except where indicated otherwise. [b] Single-point calculations at QCISD geometries, ΔZPE taken from vibrational analysis at the QCISD level, except where indicated. [c] Wrong dissociation behavior; see text. [d] ROHF wave function, unstable to symmetry breaking, collapses to CC. [e] UHF does not converge outside C_2 symmetry; therefore, (numerical) UQCISD second derivative calculations were impossible; ΔZPE taken from B3LYP calculations. [f] At B3LYP geometry and with ΔZPE from B3LYP vibrations. [g] Could not be located because of ROHF symmetry breaking in LC1. [h] Minimum at QCISD, low-lying transition state at ROHF and B3LYP (*cf.* Figure 8 and text). [i] Minimum at ROHF, transition state at all other levels. [j] Total energies in hartrees. [k] At the ROHF level, rectangular CB is a transition state.[1,2] [l] At the QCISD level only, rhombic CB lies 0.75 kcal/mol lower in energy than the rectangular structure. Listed is the energy and ZPE for the latter. [m] Zero-point vibrational energies in kilocalories per mole. In the ΔE_0 columns, the ZPEs relative to that of rectangular CB are added to ΔE. [n] Taken from QCISD calculation.

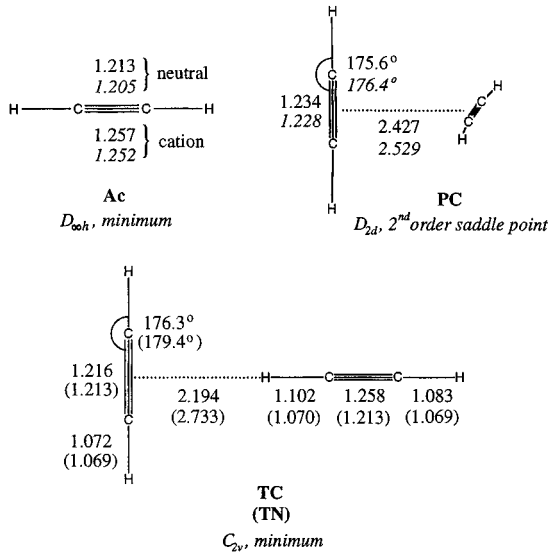

Figure 5. Geometries of Ac, Ac$^{\bullet+}$, TC, TN (in parentheses), and PC optimized by QCISD/6-31G* (normal) and B3LYP/6-31G* (italic). *Cf.* Table 2 for energies.

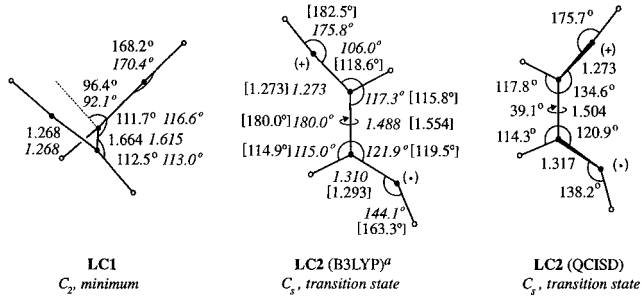

Figure 6. Geometries of the linear complexes, LC1 and LC2, optimized by QCISD/ 6-31G* (normal) and B3LYP/6-31G* (italic). [a]Numbers in brackets are for the QCISD second order saddle point (see text). *Cf.* Table 3 for energies.

substantially overestimated, which is another expression of the wrong dissociation behavior.

3.3. Tightly Bonded Complexes. Although PC is a shallow energy minimum at the ROHF level (*cf.* Figure 2), it turns into a second order saddle point at all other levels, where (under maintenance of C_2 symmetry) *both* imaginary modes lead to the same new structure.[38] It corresponds to a "linear complex" LC1 (*cf.* Figure 6) analogous to that found previously for (ethylene)$_2^{\bullet+}$;[3] *i.e.*, it has one long (≈1.66 Å) and two short C−C bonds (≈1.27 Å)[39a,b] and a rather flat surface for rotation around the long bond (Figure 7). At the CCSD(T)/cc-pVTZ level the equilibrium conformation of LC1 lies ≈5 kcal/mol below PC in energy (*cf.* Tables 2 and 3).

At correlated levels (B3LYP, QCISD) LC1 is a shallow potential energy minimum, but the nature of this complex is different at the HF level. Although it is possible to find an (apparent) potential energy minimum corresponding to LC1 within C_2 symmetry by ROHF, this lies 1.35 kcal/mol *above* PC (which is why PC is a minimum at this level). Also, it turns out that the ROHF wave function is unstable to symmetry breaking and relaxes to one where spin and charge are localized on opposite ends of the molecule; hence, LC1 is not a true energy minimum. By UHF, LC1 lies 7.8 kcal/mol below PC, but it is a transition state.

On relaxing the geometry of LC1 at the HF level, a second long bond to a vicinal C atom begins to form so that a three-membered ring complex results. As spin and charge in this new species are largely localized on the exocyclic CH unit, it may be viewed as the radical cation of a cyclopropenylcarbene (CC), which will be considered in more detail below. However, before doing this, we should point out that at the HF level, under certain conditions, LC1 is found to relax to another linear complex whose wavefunction resembles that obtained at the ROHF level upon symmetry breaking. In this species, which we shall call LC2, the spin-carrying end resembles a vinyl radical (bent, $R_{C=C} \approx 1.31$ Å) and the opposite end a vinyl cation (linear, $R_{C=C} \approx 1.27$ Å). It corresponds to the structure which Booze and Baer obtained on UHF/3-21G geometry optimization

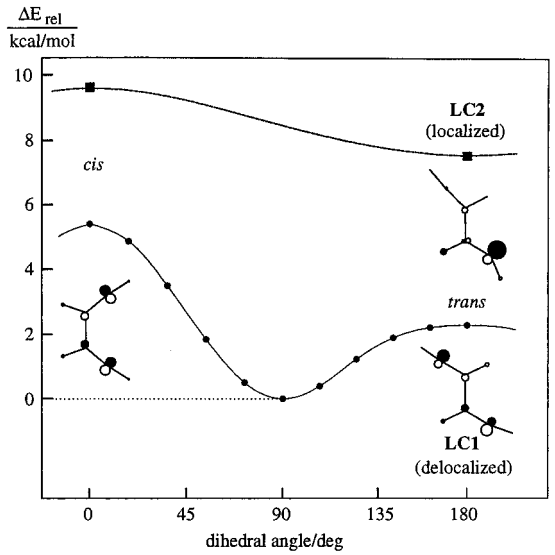

Figure 7. Potential surface for rotation around the central bond in LC1 and LC2 according to B3LYP/6-31G* calculations. Each filled symbol corresponds to a fully optimized geometry. Insets show the shape of the HOMOs at the *trans* and *cis* geometry of the localized (LC1) and delocalized state (LC2).

of the acetylene *trimer* cation (after loss of a neutral monomer).[16,39c]

At correlated levels, however, LC2 lies *higher* in energy than LC1 and collapses to the latter (or, bypassing LC1, to CC) on unconstrained geometry optimization. Apparently, correlation reverts the preference of the HF calculations for linear complexes with localized spin and charge. However, a careful search of the B3LYP potential energy surface in the vicinity of the LC2 structure revealed a region with a negative eigenvalue of the Hessian, which permitted reaching a first order saddle point. Following the imaginary normal mode showed that this structure corresponds to a planar transition state for shifting one of the central H-atoms to the vinyl cation carbon (see Figure 6), which yields a structure MA whose significance will be discussed in the following section on stable $C_4H_4^{\bullet+}$ isomers.

Reoptimization of the B3LYP structure of LC2 at the QCISD level proved very difficult. On enforcing a planar *trans* conformation, a second order saddle point was reached whose geometry differs, however, significantly from the B3LYP one (*cf.* numbers in brackets in Figure 6). The imaginary mode of lowest frequency corresponded to rotation around the central bond (the other one represents the H-migration), so we followed this in an attempt to reach the true transition state for a [1,2] H-shift on the QCISD surface. However, unlike in the case of LC1 where the "relaxed" surface for rotation around the single bond can easily be calculated (Figure 7), this is not readily possible for LC2 with methods involving correlated wave functions because, once C_s symmetry is left, they tend to collapse to the delocalized LC1 (or the H-shifted product) unless the vinyl radical end is forced to remain strongly bent.

In spite of these difficulties we eventually succeeded in locating a true transition state for the [1,2] H-shift also at the QCISD level, but this turned out to have a very different dihedral angle of 39°, albeit with bond lengths and angles quite similar to the B3LYP ones (*cf.* Figure 6). Nevertheless, the CCSD(T) energy of LC2 is 1.9 kcal/mol lower at the B3LYP than that at the QCISD geometry (at B3LYP, the same energy difference is 2.8 kcal/mol). As LC2 is not a minimum, this does not necessarily indicate that B3LYP gives a better representation of the CCSD(T) surface than QCISD, but as we were not able to fully explore the QCISD surface (to find perhaps another,

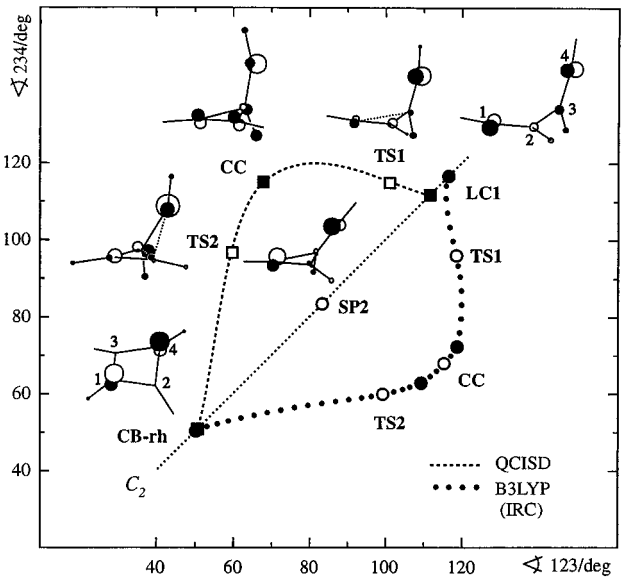

Figure 8. Reaction pathways for the decay of LC1 to (rhombic) CB via CC by B3LYP/6-31G* (dotted line connecting circles, representing an IRC pathway) and QCISD/6-31G* (dashed line connecting squares) plotted as a function of the two angles $C_1-C_2-C_3$ and $C_2-C_3-C_4$. Filled symbols denote minima; open symbols, saddle points. The diagonal line corresponds to a pathway under maintenance of C_2 symmetry which leads via a second order saddle point SP2. Insert drawings depict the change of the HOMO along the reaction.

lower-lying saddle point at a larger diehdral angle), we prefer to take the B3LYP geometry as a reference in this case. If we do this, the LC2−LC1 energy difference (*i.e.*, the activation energy for the H-shift) amounts to 7 kcal/mol at the CCSD(T) level or 6 kcal/mol if ΔZPE is taken into account (*cf.* Table 3).

Coming back to CC, we note that this species is also formed from LC1 via a very low-lying transition state TS1. It is a shallow energy minimum of C_s symmetry by QCISD, but not by B3LYP or ROHF where it is formally a saddle point between two slightly distorted, identical CC minima. However, the surface is so flat (also by QCISD) that not too much significance should be attached to this qualitative difference.[40] More importantly, CC collapses via another very low-lying transition state (TS2) to the cyclobutadiene radical cation (CB). Figure 8 shows the pathway and the change in shape of the HOMO in the course of the LC1 → CC → CB conversion. The 0 K activation energy for the LC1 → CC conversion via TS1 is only ≈0.2 kcal/mol at the QCISD and CCSD(T) levels. Hence, LC1 and CC cannot be more than very fleeting transients in the $Ac^+ + Ac^{\bullet+}$ reaction.

If we review the pathway of the $Ac + Ac^{\bullet+}$ reaction, we note that none of the stationary points which we have found so far appear to be disposed for holding up the nearly activationless collapse to CB, as discussed in the following section. In fact, it is likely that if the dynamics of this process are taken into account, some or all of them may be bypassed entirely by most of the trajectories.

3.4. Stable $C_4H_4^{\bullet+}$ Structures and Their Formation. As mentioned above, LC1 decays via CC to CB, which comes in two nearly isoenergetic structures (rhombus and rectangle) that reside in shallow minima on the bottom of the Jahn−Teller surface of CB.[1,2] For convenience we will consider only the rhombic form, CB-rh, in the context of the CC → CB rearrangement because this is the state which correlates with CC (although this only represents the global $(CH)_4^{\bullet+}$ minimum at the QCISD level). The overall activation energy for this process is <1 kcal/mol, and the rearrangement to CB is exothermic by nearly 2 eV.[41] Thus, it seems that there is an

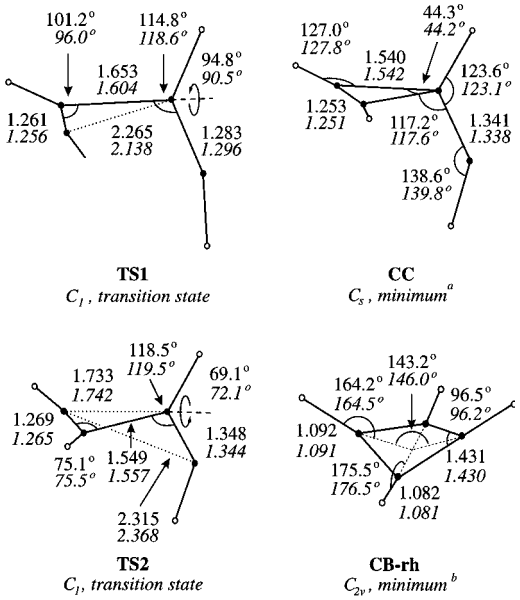

Figure 9. Geometries of the stationary points on the way from LC1 to CB by QCISD/6-31G* (normal) and B3LYP/6-31G* (italic). [a]In B3LYP, CC in C_s symmetry is a transition state connecting two slightly distorted CC structures (*cf.* Figure 8 and Supporting Information).[40] [b]CB-rh (rhombic CB) is the lowest energy $(CH)_4^{\bullet+}$ structure by QCISD, but by B3LYP/6-31G* and CCSD(T)/cc-pVTZ//QCISD/6-31G* this lies 2.1 and 1.6 kcal/mol, respectively, above the rectangular structure.[2]

almost continuous downhill pathway which connects Ac + $Ac^{\bullet+}$ with CB, which is indeed the product which is observed in condensed-phase reactions, *i.e.*, under conditions of rapid excess energy dissipation.

However, in the high-pressure gas phase experiments,[12] two distinct $C_4H_4^{\bullet+}$ populations were observed, one of which was assigned to the vinylacetylene radical cation (VA), so we must also consider pathways leading to other isomers. In our above search for LC2 we had found that this is a transition state which leads from LC1 to a linear species with a shifted H-atom which may be viewed as the radical cation of methyleneallene $CH_2{=}C{=}CHCH^{\bullet+}$ (MA). This has the same C/H connectivities as methylenecyclopropene (MCP), which is over 30 kcal/mol more stable. Indeed, the transition state connecting the two species (TS3) lies only ≈4 kcal/mol above MA. Thus, the final part of a pathway leading to one other isomeric cation, MCP, was identified.[42]

The remaining two other stable $C_4H_4^{\bullet+}$ species, *i.e.*, the radical cations of butatriene (BT) and vinylacetylene (VA), require an additional hydrogen shift to be formed from MA. Thus, we located the transition state TS4 for shifting the single allenic hydrogen in MA to the carbenic carbon to give BT as well as that for shifting the same hydrogen to the central allenic carbon to give VA, *i.e.*, TS5. The corresponding structures are depicted in Figure 10, while Figure 11 shows the change in the FMOs during the decay of MA to the three stable isomers. There one can see how H-shifts are promoted by localization of the LUMO in a single p AO (or sp hybrid). Note that the FMOs at the transition states do not necessarily correlate with those in the products; *i.e.*, some major changes in the wave functions may still occur in the downhill parts of the potential energy surfaces.

Our earlier observation that the linear complex between ethylene and its radical cation decays preferentially by a [1,3] hydrogen shift[3] incited us to search also for an analogous pathway which would connect LC1 (or LC2) directly to VA. We succeeded indeed in finding a corresponding transition state on the B3LYP surface, but as this turned out to be >1 eV above TS5, we did not explore this any further.

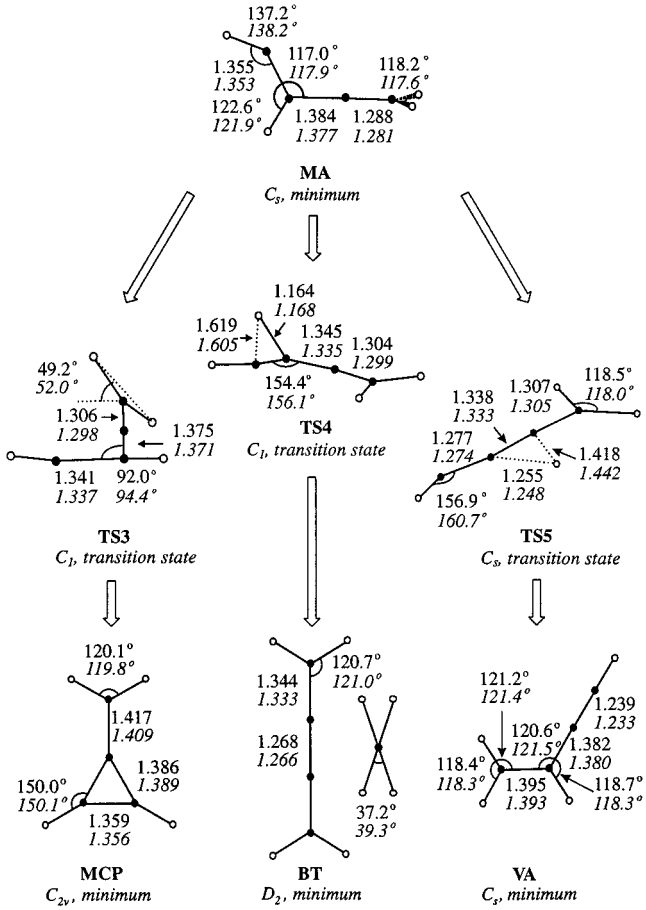

Figure 10. Geometries of the stable $C_4H_4^{\bullet+}$ isomers butatriene (BT), vinylacetylene (VA), and methylenecyclopropane (MCP), as well as the transition states for their formation from methyleneallene (MA) by QCISD/6-31G* (normal) and B3LYP/6-31G* (italic).

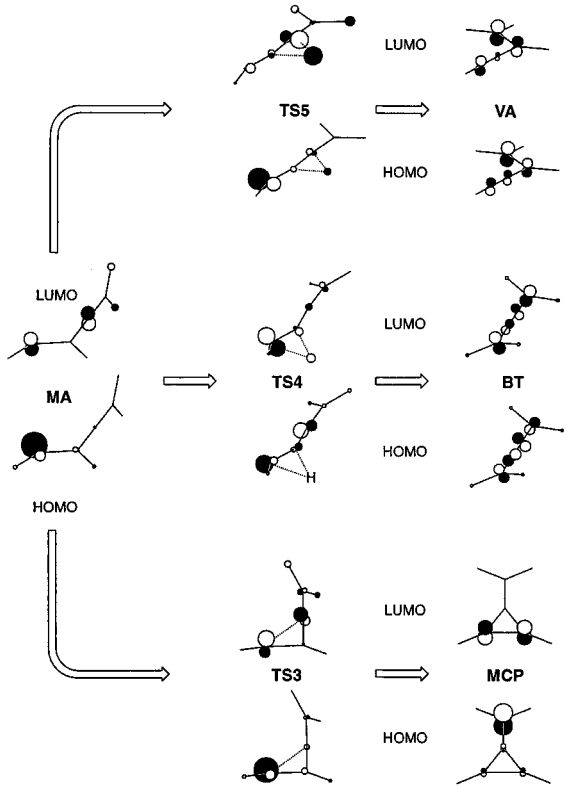

Figure 11. Change in the shape of the frontier molecular orbitals (FMOs) during the rearrangements of MA to MCP, BT, and VA, respectively.

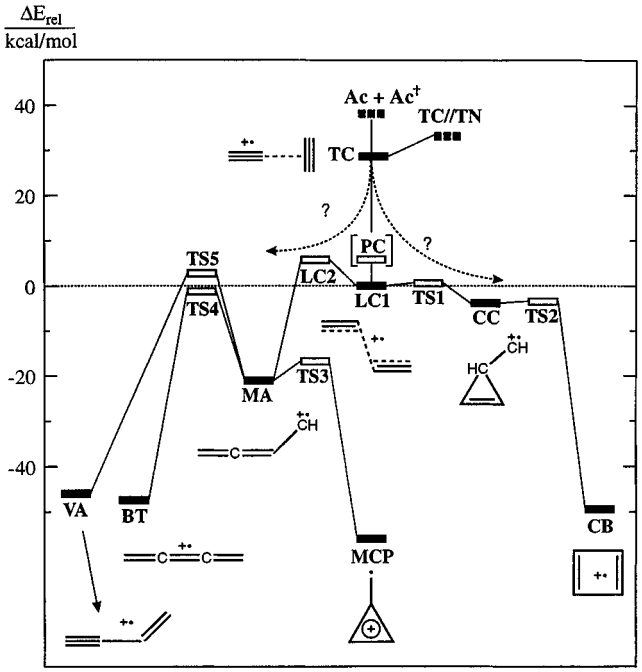

Figure 12. Schematic potential energy diagram for the Ac + $Ac^{\bullet+}$ reaction and the ensuing decay to stable $C_4H_4^{\bullet+}$ isomers, based on CCSD(T)/cc-pVTZ energies (for the corresponding 0 K energies; see Table 3). Solid bars represent minima; open bars, transition states. At the CCSD(T)/cc-pVTZ level the equilibrium structure of LC1 lies 5.7 kcal/mol below PC (*cf.* Tables 2 and 3)

We are now in a position to compare the activation energies for the formation of all four stable $C_4H_4^{\bullet+}$ isomers from LC1, the primary product of the reaction of Ac + $Ac^{\bullet+}$ (see Figure 12). Firstly, we note that the rearrangement of this to CB, which retains the C−H connectivities of the incipient complex, is nearly activationless (*cf.* Figure 8). Conversely, formation of the other isomers involves hydrogen shifts which appear to be mediated by a localization of spin and charge, thus creating an empty p AO for "accepting" the migrating H atom. This localization to form LC2 occurs spontaneously at the HF level, but the entailing reduction in electron correlation seems to make this an uphill process in the final analysis (by ≈7 kcal/mol by CCSD(T)/cc-pVTZ), thus putting the ensuing rearrangements at a disadvantage relative to the decay to CB.

Among these rearrangements which occur all via the allenic carbene cation MA, the most favorable one is again that which requires no further H shifts, *i.e.*, the collapse to MCP via TS3 (E_a = 3.2 kcal/mol from MA), which furthermore turns out to be the most stable of all $C_4H_4^{\bullet+}$ isomers. Of the two [1,2] hydrogen shifts which lead to the linear structures, the one giving BT via TS4 (E_a = 16.9 kcal/mol from MA) wins against the other one via TS5 to VA (E_a = 20.5 kcal/mol).

Note that the order of stabilities of the four stable $C_4H_4^{\bullet+}$ isomers is different than that of the parent neutral compounds. For the sake of comparison we have calculated the energies of *neutral* VA, BT, CB, and MCP by the same methods we had used for the radical cations. These results are gathered in Table 4, while the structures are displayed in Figure 13. If we take the CCSD(T)/cc-pVTZ numbers as a reference, then we note that the ≈8 kcal/mol destabilization of butatriene relative to vinylacetylene is in reasonable agreement with the experimental estimate of an ≈10 kcal/mol enthalpy difference between the two compounds.[43] Also, the ≈9 kcal/mol destabilization of cyclobutadiene relative to methylenecyclopropane is within 1 kcal/mol of a recent G2 calculation.[44,45]

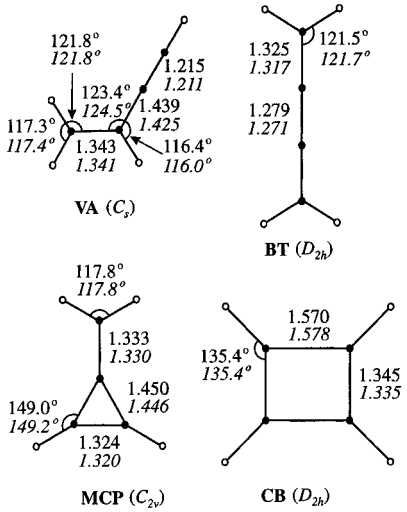

Figure 13. Geometries of stable *neutral* C_4H_4 isomers by QCISD/6-31G* (normal) and B3LYP/6-31G* (italic).

TABLE 4: Energies (kcal/mol) of *Neutral* C_4H_4 Structures[a] Relative to VA

neutral C_4H_4 structure	B3LYP/6-31G*		QCISD/6-31G*		CCSD(T)/cc-pVTZ[b]	
	ΔE	ΔE_0	ΔE	ΔE_0	ΔE	ΔE_0
BT	1.91	*1.56*	9.02	*8.73*	8.19	*7.90*
MCP	20.39	*20.24*	24.60	*24.77*	24.39	*24.55*
CB	36.61	*36.62*	34.83	*34.78*	33.74	*33.69*
VA E[c]	−154.733 80		−154.238 22		−154.444 27	
ZPE[d]	38.39		38.23		(38.23)	

[a] For B3LYP and QCISD optimized structures see Figure13. [b] Single point calculations at QCISD geometries; ΔZPE taken from vibrational analysis at the QCISD level. [c] Total energies in hartrees. [d] Zero-point vibrational energies in kilocalories per mole. In the ΔE_0 columns, the ZPEs relative to that of VA are added to ΔE.

Finally, we caution that our exploration of the $C_4H_4^{\bullet+}$ potential energy surface is by no means complete in that we have only probed pathways connecting equilibrium structures (minima) via transition states (saddle points). We cannot exclude that some of the potential energy "valleys" have *bifurcations* which may result in competing processes that elude our attention. In particular it is conceivable that in the course of the decay of the loose complex, TC, structures with localized spin and charge such as LC2 may be formed directly, *i.e.*, without prior delocalization as in PC or LC1. Such pathways could for example provide access to H-shifted isomers in competition with the decay to CB. However, such bifurcations are nearly impossible to locate, and, even if they could be found, quantitative predictions would require dynamics calculations because standard kinetics are no longer valid in such regions of phase space. This is outside the scope of this work but could be a challenging field for future investigations.

3.5. Performance of the B3LYP Method. Although DFT methods are rapidly entering the mainstream of computational chemistry, there is still a need to test them in different fields of application. It is in this perspective that we have carried out the entire search of the $C_4H_4^{\bullet+}$ potential energy surface also by the B3LYP method, which in our's and other's experience has proven to be overall the most reliable of the current DFT models (others may be better for specific applications).

We had already noted in previous sections a somewhat unexpected success of B3LYP in that its modeling of the weakly bound neutral acetylene dimer proved to be in excellent accord with experiment and with high-level coupled cluster calculations. Surprisingly the best agreement was obtained with the 6-31G*

basis set which may be due to a fortuitous cancellation of errors but shows that the results obtained with this method cannot be systematically improved by going to large basis sets. Conversely, weakly bound ion−molecule complexes cannot be described correctly by the B3LYP method due to its wrong asymptotic behavior which results in a failure to localize the spin and/or the charge on dissociation, as elaborated in section 3.2. However, once one comes to the tightly bound regime where spin and charge are delocalized, the description is again correct.

Generally, B3LYP/6-31G* gives structures and energies in close agreement with our reference level of theory, *i.e.*, CCSD(T)/cc-pVTZ energies at QCISD/6-31G* geometries (*cf.* Figures 5, 6, 9, and 10 and Table 3), except for "soft" coordinates in long-bond complexes (*i.e.*, the angles in LC1) or transition states (*i.e.*, the twisting angle of the CH_2 group in TS3). Interestingly, the greatest discrepancies in the energies are to be found among the stable $C_4H_4^{\bullet+}$ isomers: whereas the reference calculations predict BT to be about 8 kcal/mol less stable than MCP, this difference is only some 3 kcal/mol in B3LYP. This testifies to the overestimation of the stability of cumulenes by this method which is already borne out in the parent neutral compounds (see Table 4). The same is true for VA relative to MCP, but to a slightly lesser degree (2 kcal/mol difference).

This does not appear to affect activation energies for H shifts which are generally within a kilocalorie permole of each other in B3LYP and the reference calculations. Conversely, the activation energies for C−C bond formation such as it occurs in LC1 → CC are too high by B3LYP compared to our reference level.

Nevertheless we note that B3LYP does an excellent job of modeling the potential energy surface on which the various $C_4H_4^{\bullet+}$ rearrangements take place, and it does this at a small fraction of the cost of the coupled cluster/QCI calculations. This should be seen in particular in the light of the fact that the usual MP2 methods (restricted or unrestricted) invariably fail in one or the other region of the surface due to symmetry breaking of the reference ROHF wave function or to excessive spin contamination of the UHF wave function which cannot be rectified at the second order level of perturbation theory.

4. Conclusions

We have investigated the reaction of acetylene (Ac) with its radical cation ($Ac^{\bullet+}$) at the CCSD(T)/cc-pVTZ//QCISD/6-31G* level of theory. Thereby we find that, once Ac and $Ac^{\bullet+}$ have approached to less than about a 3 Å center to center distance, spin and charge begin to delocalize and the complex collapses smoothly to the cyclobutadiene radical cation (CB) via a linear complex LC1 and/or a cyclopropenylcarbene cation, CC. Although spin and charge relocalize partially in the course of this process, they do this mainly in transition states where the resulting loss in correlation energy is compensated by the energy for formation of new C−C bonds.

Conversely, this is not the case in the transition states for H-shifts which are required for the formation of other stable $C_4H_4^{\bullet+}$ isomers. In particular, localization of the charge in the primary intermediate LC1, which leads to creation of an empty p AO for accepting a migrating H-atom, entails a 0 K energy barrier of ≈6 kcal/mol. Hence, collapse of Ac + $Ac^{\bullet+}$ under maintenance of the $(CH)_4$ connectivity is favored over processes leading to rearranged isomers. Among those, collapse of the pivotal intermediate, MA, to the methylenecyclopropane radical cation (MCP), the most stable $C_4H_4^{\bullet+}$ isomer, is strongly favored over processes leading to the linear conjugated isomers, *i.e.*, the radical cations of butatriene (BT) and vinylacetylene (VA).

The above findings are in accord with condensed phase experiments on alkylated acetylenes where the corresponding CB derivatives were the only products observed. However, in gas phase studies other parts or the potential energy surface appear to be accessed (*cf.* Introduction). Our results suggest that this would need to involve a bypassing of the minimum energy pathways explored in this study. In particular, if a potential energy valley leading to a product with delocalized spin and charge (such as LC1) would contain a bifurcation directed toward a structure with localized charge that is well-disposed for H migration, this could result in competitive rearrangements to non-$(CH)_4$ isomers.

The exploration of such mechanisms is outside the scope of this work which should therefore serve to lay the basis for future experimental and computational work. In particular, a reexamination of the products of the Ac + $Ac^{\bullet+}$ reaction in an ion flow tube would appear to be an attractive target of investigation in view of the present results which put rearrangement to VA (which was reported to have been observed by Knight *et al.*[12]) at a considerable disadvantage relative to other processes.

Acknowledgment. This work has been funded through Grant No. 2028-047212.96/1 of the Swiss National Science Foundation and is part of a joint project between the University of Fribourg (Institute of Physical Chemistry) and the Academy of Sciences of the Czech Republic (J. Heyrovsky Institute), respectively, under COST action D3 (Theory and Modeling of Chemical Systems and Processes) funded in Prague by the Ministry of Education of the Czech Republic. We thank the Swiss Center for Scientific Computing in Manno for a generous allocation of CPU time on the NEC SX-3 without which the coupled cluster calculations would have been impossible to carry out.

Supporting Information Available: Tables listing absolute energies and cartesian coordinates for all stationary points located in this study (12 pages). Ordering information is given on any current masthead page.

References and Notes

(1) Part 1: Roeselová, M.; Bally, T.; Jungwirth, P.; Cársky, P. *Chem. Phys. Lett.* **1995**, *234*, 395.

(2) Part 2: Hrouda, V.; Bally, T. *J. Phys. Chem. A* **1997**, *101*, 3918.

(3) Jungwirth, P.; Bally, T. *J. Am. Chem. Soc.* **1993**, *115*, 5783.

(4) (a) Courtneidge, J. L.; Davies, A. L. *Acc. Chem. Res.* **1987**, *20*, 90, and ref 23−27 cited therein. (b) Shiotani, M.; Ohta, K.; Nagata, Y.; Sohma, J. *J. Am. Chem. Soc.* **1985**, *107*, 2562.

(5) (a) Badger, B.; Brocklehurst, B. *Trans. Faraday Soc.* **1969**, *65*, 2576, 2582, 2588. (b) Chikai, Y.; Yamamoto, Y.; Hayashi, K. *Bull. Chem. Soc. Jpn.* **1988**, *61*, 2281.

(6) Tachikawa, H.; Shiotani, M.; Ohta, K. *J. Phys. Chem.* **1992**, *96*, 164.

(7) (a) See: Field, F. H.; Franklin, J. L.; Lampe, F. W. *J. Am. Chem. Soc.* **1957**, *79*, 2665. (b) Most pertinent references of the work up to 1982 are summarized by Ono and Ng[8a] (ref 1−22).

(8) (a) Ono, Y.; Ng, C. Y. *J. Chem. Phys.* **1982**, *77*, 2947. (b) Ono, Y.; Ng, C. Y. *J. Am. Chem. Soc.* **1982**, *104*, 4752.

(9) See, e.g.: (a) Munson, M. S. A. *J. Phys. Chem.* **1965**, *69*, 572. (b) Derwish, G. A. W.; Galli, A.; Giardini-Guidoni, A.; Volpi, G. G. *J. Am. Chem. Soc.* **1965**, *87*, 1159.

(10) Smyth, K. C.; Lias, S. G.; Ausloos, P. *Combust. Sci. Technol.* **1982**, *28*, 147.

(11) See e.g.: Omont, A. *Astron. Astrophys.* **1986**, *164*, 159. Allamandola, L. J.; Tielens, A. G.; Barker, J. R. *Astrophys. J.* **1985**, *290*, L25.

(12) Knight, J. S.; Freeman, C. G.; McEwan, M. J.; Anicich, V. G.; Huntress, W. T. *J. Phys. Chem.* **1987**, *91*, 3898.

(13) Wagner-Redeker, W.; Illies, A. J.; Kemper, P. R.; Bowers, M. T. *J. Am. Chem. Soc.* **1983**, *105*, 5719.

(14) Zhang, M.-Y.; Wesdemiotis, C.; Marchetti, M.; Danis, P. O.; Ray, J. C.; Carpenter, B. K.; McLafferty, F. W. *J. Am. Chem. Soc.* **1989**, *111*, 8341;. Zhang, M.-Y.; Carpenter, B. K.; McLafferty, F. W. *J. Am. Chem. Soc.*, **1991**, *113*, 9499.

(15) Shay, B. J.; Eberlin, M. N.; Cooks, R. G.; Wesdemiotis, C. *J. Am. Soc. Mass Spectrom.* **1992**, *3*, 518.

(16) Booze, J. A.; Baer, T. *J. Chem. Phys*, **1993**, *98*, 186.

(17) A few years earlier, Shinohara et al. had obtained $(C_2H_2)_n^{\bullet+}$ (n = 2−4) by photoionization of mixed $(Ar)_n(C_2H_2)_m$ clusters.[18] These authors claimed that in their experiments the ionized acetylene clusters were stabilized by evaporation of Ar atoms. However, Booze and Baer argue that the evidence for this mechanism is not conclusive and that the ionized clusters might just as well have been stabilized by loss of neutral acetylenes.[16]

(18) Shinohara, H.; Sato, H.; Washida, N. *J. Phys. Chem.* **1990**, *94*, 6718.

(19) Zhu, Y. F.; Allman, S. L.; Phillips, R. C.; Garrett, W. R.; Chen, C. H. *Chem. Phys. Lett.* **1994**, *224*, 7.

(20) For a description of the density functionals as implemented in the Gaussian series of programs, see: Johnson, B. G.; Gill, P. M. W. L.; Pople, J. A. *J. Chem. Phys.* **1993**, *98*, 5612.

(21) Quadratic configuration interaction with single and double substitutions based on a UHF reference wave function (Pople, J. A.; Head-Gordon, M.; Raghavachari, K. *J. Chem. Phys.* **1987**, *87*, 5968).

(22) Hariharan, P. C.; Pople, J. A. *Theor. Chim. Acta* **1973**, *28*, 213.

(23) Gonzales, C.; Schlegel, H. B. *J. Chem. Phys.* **1989**, *90*, 2154; *J. Phys. Chem.* **1990**, *94*, 5523.

(24) Coupled cluster calculation accounting for single and double excitations (see e.g.: Bartlett, R. J. *J. Phys. Chem.* **1989**, *93*, 1697, and references cited therein), augmented by a quasi-perturbative estimate for triple excitations (Raghavachari, K.; Trucks, G. W.; Pople, J. A.; Head-Gordon, M. *Chem. Phys. Lett.* **1989**, *157*, 479).

(25) Dunning, T. H. *J. Chem. Phys.* **1989**, *90*, 1007.

(26) Boys, S. F.; Bernardi, F. *Mol. Phys.* **1970**, *19*, 553.

(27) Stanton, J. F. *J. Chem. Phys.* **1994**, *101*, 371. See also: Watts, J. D.; Gauss, J.; Bartlett, R. *J. Chem. Phys.* **1993**, *98* , 1993.

(28) Frisch, M. J.; Trucks, G. W.; Schlegel, H. B.; Gill, P. M. W.; Johnson, B. G.; Robb, M. A.; Cheeseman, J. R.; Keith, T.; Petersson, G. A.; Montgomery, J. A.; Raghavachari, K.; Al-Laham, M. A.; Zakrzewski, V. G.; Ortiz, J. V.; Foresman, J. B.; Cioslowski, J.; Stefanov, B. B.; Nanayakkara, A.; Challacombe, M.; Peng, C. Y.; Ayala, P. Y.; Chen, W.; Wong, M. W.; Andres, J. L.; Replogle, E. S.; Gomperts, R.; Martin, R. L.; Fox, D. J.; Binkley, J. S.; DeFrees, D. J.; Baker, J.; Stewart, J. P.; Head-Gordon, M.; Gonzalez, M.; Pople, J. A. *Gaussian 94* (Revision B .1); Gaussian, Inc.: Pittsburgh, PA, 1995.

(29) (a) Prichard, D. G.; Nandi, R. N.; Muenter, J. S. *J. Chem. Phys.* **1988**, *89*, 115. (b) Fraser, G. T.; Suenram, R. D.; Lovas, F. J.; Pine, A. S.; Hougen, J. T.; Lafferty, W. J.; Muenter, J. S. *J. Chem. Phys.* **1988**, *89*, 6028. (c) Alberts, I. L.; Rowlands, T. W.; Handy, N. C. *J. Chem. Phys.* **1988**, *89*, 3811.

(30) Van der Waals systems: Hobza, P.; Sponer, J.; Reschel, T. *J. Comput. Chem.* **1995**, *16*, 1315. H-bonded complexes: Del Bene, J. E.; Person, W. B.; Szczepaniak, K. *J. Phys. Chem.* **1995**, *99*, 10705.

(31) Handy, N. C.; Murray, Ch. W.; Amos, R. D. *J. Phys. Chem.* **1993**, *97*, 4392.

(32) With this method, the π_g and π_u bending frequencies of acetylene are 653 (expt, 624 cm^{-1}) and 768 (expt, 747 cm^{-1}). Note also that, at this level, the frequency corresponding to the intermolecular rotation was only 23 cm^{-1} and the intermolecular stretch 56 cm^{-1} which testifies to the flatness of the potential surface and the ease of automerization of TN.

(33) See e.g.: Badger, B.; Brocklehurst, B. *Trans. Faraday Soc.* **1966**, *66*, 2939.

(34) Note, however, that in some cases, hydrogen-bonded structures may be preferred over sandwich-type dimer cations. See e.g. the work on $(benzene)_2^{\bullet+}$: Hiraoka, K.; Fujimaki, S.; Aruga, K. *J. Chem. Phys.* **1991**, *95*, 8413, and references cited therein.

(35) A reviewer has pointed out the alternative possibility of ionization from a σ-MO of TN which would yield a complex between a HCC radical and (nonclassical) protonated Ac:

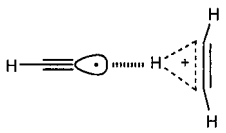

However, ΔH^{298} for the reaction $C_2H_2^{\bullet+} + C_2H_2 \rightarrow HCC^{\bullet} + C_2H_3^+$ is 29.5 kcal/mol [derived from DH^{298}(HCC−H) = 132.8 kcal/mol (Berkowitz, J.; Ellison, G. B.; Gutman, D. *J. Phys. Chem.* **1994**, *98*, 2744) plus $I(H^{\bullet})$ = 13.6 eV minus $I(C_2H_2)$ = 11.4 eV minus PA(C_2H_2) = 154 kcal/mol (Lossing, T. A., *Can. J. Chem.* **1971**, *49*, 357)], which puts this state at a strong energetic disadvantage, even if the binding energy between $HCC^{\bullet}$ and $C_2H_3^+$ should be unusually high (optimization of this complex within C_{2v} symmetry led to a second order saddle point only 1 kcal/mol below $HCC^{\bullet} + C_2H_3^+$.

(36) We found that this behavior is general and an inherent property of all density functionals which we could test: the dissociation curve for $H_2^{\bullet+}$ also falls off in the region where localization to form $H^{\bullet}$ and H^+ should occur and converges eventually to a value below the binding energy of $H_2^{\bullet+}$! This must be due to the fact that the exchange parts of the functionals show a wrong asymptotic behavior, as shown recently by model calculations (Filippi, L.; Umrigar, C. J.; Taut, M. *J. Chem. Phys.* **1994**, *100*, 1290) or by calculations on charge transfer complexes (Ruiz, E.; Salahub, D. R.; Vela, A. *J. Phys. Chem.* **1996**, *100*, 12265).

(37) (a) CI with all singly and doubly excited configurations. In order to avoid possible problems with perturbative methods based on reference wavefunctions which may be far from the correlated ones, we preferred this fully variational procedure in this case. (b) Note that the energy of PC relative to the separated fragments is strongly underestimated by CISD due to the size inconsistency of this procedure.

(38) This peculiar feature of PC is due to the fact that one can form four equivalent linear complexes from a perpendicular complex of D_{2d} symmetry (actually PC is a "degenerate" transition state for their pairwise automerization).

(39) (a) Note that the bond lengths of LC1 (*cf.* Figure 6) are quite different from those reported in ref 16 for the corresponding structure 7(b). Whereas the long bond distance depends very strongly on the basis set (1.79 by 3-21G, 1.70 by 6-31G*) and is reduced by ≈0.05 Å by correlation, a recalculation of LC1 by UHF/3-21G showed that the short bond length given in ref 16 is too short by ≈0.1 Å. (b) Booze and Baer reported their structure 7(b) (our LC1) to be an energy minimum at the UHF/3-21G level. We confirmed this but found that, on going to UHF/6-31G*, it turns into a transition state with an imaginary mode pointing toward CC to which it collapses spontaneously. By ROHF/6-31G* it remains a minimum which is, however, a meaningless result due to the instability of the ROHF wave function. (c) Their structure 7e corresponds to the cis-conformation of LC2 which is a local minimum at the UHF/3-21G level.

(40) Note that there are two possible conformations of CC. The one shown in Figure 9 has the H atom at the "carbenic" center facing the three-membered ring, whereas in another (nearly isoenergetic) one that H atom faces the opposite way. It is the first structure which is formed in the LC1−TS1−CC rearrangement, but both conformers of CC decay with similar activation energies to CB. At the B3LYP/6-31G* level, the rotational barrier for interconversion of the two conformers is 3.2 kcal/mol.

(41) Note that the direct conversion of LC1 to CB under maintenance of C_2 symmetry leads via a second order saddle point (SP2 in Figure 8) and is therefore not competitive with the reaction via CC.

(42) A reviewer has asked us to compute the 298 K enthalpy of formation of MCP from the calculated enthalpy change for the reaction Ac + $Ac^{\bullet+}$ → MCP. Adding thermal corrections to 298 K from a B3LYP/cc-pVTZ calculation (*cf.* last paragraph of section 3.1) to the CCSD(T)/cc-pVTZ energy difference of 94.71 kcal/mol yields a reaction enthalpy of 91.5 kcal/mol. Adding to this $\Delta_f H^{298}$(Ac) = 54.5 kcal/mol and $\Delta_f H^{298}(Ac^{\bullet+})$ = 317.4 kcal/mol[43] yields $\Delta_f H^{298}$(MCP) = 280.4 kcal/mol.

(43) Lias, S. G.; Bartmess, J. E.; Liebman, J. F.; Holmes, J. L.; Levin, R. S.; Mallard, W. G. *Gas Phase Ion and Neutral Thermochemistry*; American Chemical Society: Washington, DC, 1988 (*J. Phys. Chem. Ref. Data* **1988**, *17*, Suppl. No. 1).

(44) Rodgers, D. W.; McLafferty, F. J.; Podosenin, A. V. *J. Phys. Chem.* **1996**, *100*, 17148.

(45) With addition of the thermal corrections up to 298 K from the QCISD calculations and on the basis of $\Delta_f H^{298}$(VA) = 73 kcal/mol,[43] we obtain $\Delta_f H^{298}$(BT) = 81.8, $\Delta_f H^{298}$(MCP) = 97.4, and $\Delta_f H^{298}$(CB) = 107.3 kcal/mol (the abbreviations refer to the *neutral* compounds). The value of MCP is in reasonable accord with the G2 value of 94 kcal/mol obtained via the enthalpy of hydrogenation to methylenecyclopropane,[44] whereas $\Delta_f H^{298}$(CB) is 6.2 kcal/mol higher than the G2 value calculated form the enthalpy of hydrogenation to cyclobutene[44] or from homodesmotic bond separation reactions (Glukhovtsev, M. N.; Laiter, S.; Pross, A. *J. Phys. Chem.* **1995**, *99*, 6828). It could be that $\Delta_f H^{298}$(VA) on which the above numbers are based is too low.